Experimental and Numerical Investigations of Al/Mg Compound Specimens under Load in an Extended Temperature Range

Thomas Lehmann
Scientific Assistant
Chemnitz University of Technology
Faculty of Mechanical Engineering

Martin Stockmann
Head of the Section Experimental Mechanics
Chemnitz University of Technology
Faculty of Mechanical Engineering

Jochen Naumann
Professor Emeritus
Chemnitz University of Technology
Faculty of Mechanical Engineering

This work is part of a research project which has the aim to analyze the strength and fracture mechanical properties of hydrostatic coextruded aluminium/magnesium compounds. The paper presents the main results of the investigations concerning compound quality as well as loading tests with these compounds at temperatures up to 400 °C. The alloyed materials are only partially bonded or damaged while the compounds of the unalloyed materials show a completely bonded interface. The strength of the interface is calculated by using failure force values of bending tests and an FE-simulation of the stress conditions at the position of the interface. The deformation behavior is determined by using Digital Image Correlation. Both the alloyed and the unalloyed materials show high strength values at the bonded parts of the material. Futhermore, by means of the tests at high temperatures, a very good deformation behavior without crack of the interface can be demonstrated.

Keywords: *aluminium/magnesium compound, interface, bending test, bonding strength, elevated temperatures, Digital Image Correlation.*

1. INTRODUCTION

Because of the claim to develop energy-saving machines and constructions, light weight materials are becoming more and more important in a wide range of applications and branches of industry. The work, which is described in the paper, is a part of the research project that is concerned with the development, the production and the characterization of new aluminium based light weight materials and their application in reliable components. One application can be found in aluminium/magnesium compounds. The aim of a subproject is to analyze the strength and fracture mechanical properties of the interface of this new lightweight material and to create a model of the interface for numerical investigations (other part of the subproject – not described in this paper). Special conditions and parameters of the co-extrusion process are a basis for the creation of an undamaged interface. Hence, it is an important task to optimize the production process of this material. Furthermore, several tests should be created to determine the properties of the interface in an extended temperature range. These investigations are fundamental because of the subsequent processing of the semi-finished product at elevated temperatures. The results should be implemented into the numerical simulations of the production process and of the loading tests.

Received: March 2009, Accepted: March 2009
Correspondence to: Thomas Lehmann
Chemnitz University of Technology,
Straße der Nationen 62, 09111 Chemnitz. Germany
E-mail: thomas.lehmann@mb.tu-chemnitz.de

2. PRODUCTION PROCESS AND SEMI-FINISHED PRODUCT

2.1 Technology

Different technologies such as friction welding, casting, rolling, explosive plating and co-extruding [1] are applicable to produce metallic material compounds. The hydrostatic co-extrusion [2] is particularly suitable to manufacture axisymmetric material compounds. The analyzed aluminium/magnesium compounds were produced with this technology by the firm CEP GmbH, Freiberg, Germany. The principle of the technology is shown in Figure 1. The press capacity is transmitted by a pressure medium, which surrounds the bolt except the part in the die. Thus, the punch is not contacted with the bolt materials. Additionally, there is good lubrication between the die and the bolt. For this reason the friction is minimized, which can be referred to as the main advantage compared with conventional technologies like direct and indirect extrusion. Hence, by means of this technology it is possible to realize higher degrees of deformation and to improve the quality of the extruded material.

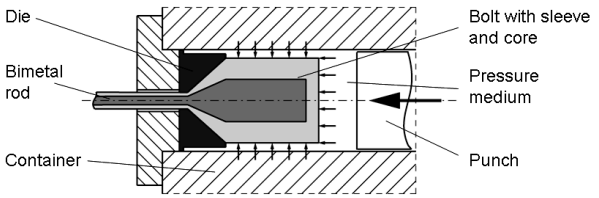

Figure 1. Principle of the hydrostatic co-extrusion process

2.2 Analyzed material

The parameters of extrusion experiments which produced the analyzed material (representative

examples) are given in Table 1. The result of the co-extrusion processes are axisymmetric semi-finished products, where pure Mg and AZ31 are used as core material. One aim was to prove the quality of the interface and to take measures to improve the production process. In addition, different tests were realized to determine mechanical properties of the compound and of the interface respectively.

Table 1. Examples of co-extrusion tests

No.	Material	D_{sleeve}/D_{core} [mm]	T_{bolt}/T_{die} [°C]	φ
1	AlMgSi1/AZ31	80/60 → 20/15	450/350	2.77
	Al99.5/Mg			
2	AlMgSi1/AZ31	80/50 → 20/12.5	300/300	2.77
	Al99.5/Mg		350/350	

In extrusion experiment 1, a wide interface (50 to 100 μm) with ramified cracks and eutectic structures was observed by a metallographic analysis of the compound of the alloyed materials, Fig. 2 [3]. By means of a micro hardness test, high values of hardness (until 300 HV 0.05) in the region of the interface were proved. These analyses were realized by the Chair of Composite Materials, Chemnitz University of Technology. At the interface of the unalloyed basic materials, only a few hard and damaged sections were found. Furthermore, it was demonstrated that the interface is melting at temperatures of 435 °C. This is one of the melting temperatures of the eutectic mixtures at the Mg-Al phase diagram (32 % Mg). This allows the conclusion that the interface was produced by a melting process during the co-extrusion because of high temperatures and subsequent cooling.

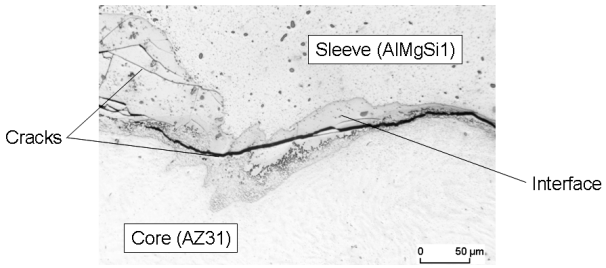

Figure 2. Interface microstructure of AlMgSi1/AZ31 – extrusion test 1 [Chair of Composite Materials]

The bolt and die temperature for extrusion test 2 were estimated by means of a numeric simulation [4] of the co-extrusion process to ensure that temperatures of 435 °C and above do not occur. These numeric simulations were realized by the Chair of Virtual Technologies, Chemnitz University of Technology, within the framework of the other part of the described subproject. For extrusion experiment 2, the temperature of bolt and die was reduced to 300 °C (alloyed material) and 350 °C (unalloyed material). A metallographic analysis shows that eutectic mixtures do not occur any longer. Thus, it seems that the temperature of 435 °C was not reached. The microstructure of the transition area shows now a narrow interface without melted structures. In the case of the co-extruded alloyed materials (AlMgSi1/AZ31), a partially bonded compound occurs [3]. The two metals are bonded only on one side of the circumference of the interface. The unbounded parts in the middle of the co-extrusion rod take approximately 30 to 40 % of the circumference. Additionally to the metallographic investigations, the cracks (unbounded parts) were detected by dye penetrant tests and ultrasonic analyses. It can be shown that the results of the different crack detection methods correlate well. A typical result of the dye penetrant tests with the compound of the alloyed materials is given in Figure 3. The penetrant which is filling the cracks and gaps is drawing on the surface (Fig. 3, grey areas) by a special developer afterwards. An example for the results of the ultrasonic tests (analysis of a 100 mm part of the bimetal rod) is shown in Figure 4. Low amplitudes of ultrasonic signal indicate a bonded area, high values show an unbounded area. The compound of the unalloyed materials is completely bonded.

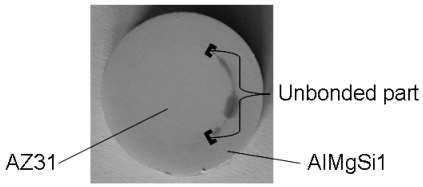

Figure 3. Crack detection by dye penetrant test, alloyed material of extrusion test 2

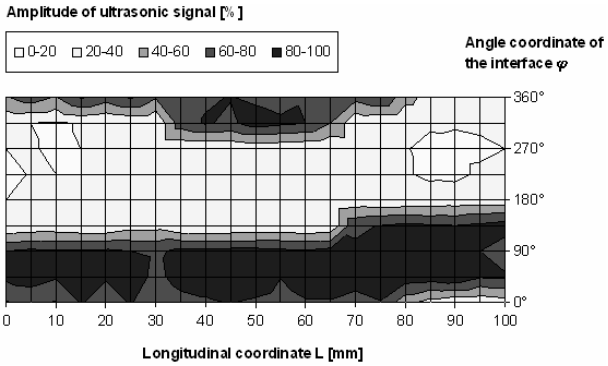

Figure 4. Example for the ultrasonic crack analyses, alloyed material of extrusion test 2

3. PUSH OUT TESTS AT ROOM TEMPERATURE

The experiments were performed in a 100 kN ZWICK testing machine by using special loading devices. Push out tests were realized for testing the aluminium/magnesium compounds under shear stress [3]. The specimen geometry is a simple disk with a thickness of 5 mm, which is separated by eroding in cross direction of the co-extrusion rod. The principle of loading is given in Figure 5. The punch is pushing the core and the basic block is supporting the sleeve material. Therefore, the interface is shear stressed. All tests caused failure at the interface of the specimens. To reach quasi-static conditions, the loading rate was chosen very low (v_{punch} = 0.2 mm/min).

The alloyed and unalloyed materials of extrusion test 1 show different kinds of failure. Figure 6 demonstrates the force versus punch displacement for representative examples of push out tests respectively. The failure of the AlMgSi1/AZ31 compound is abrupt, almost without plastic deformation of the basic materials and is associated with high forces (about 20 kN), Figs. 6 and 7 (left). The behaviour of the compound of the unalloyed

materials (Al99.5/Mg) is characterized by failure with high plastic deformations and high forces (about 14.5 kN), Figs. 6 and 7 (right).

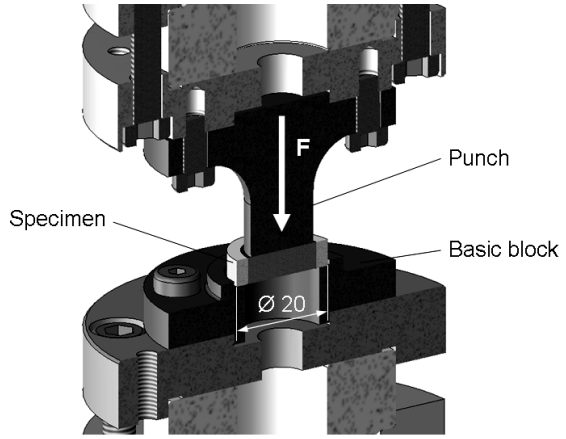

Figure 5. CAD-model of the push out test device, longitudinal section

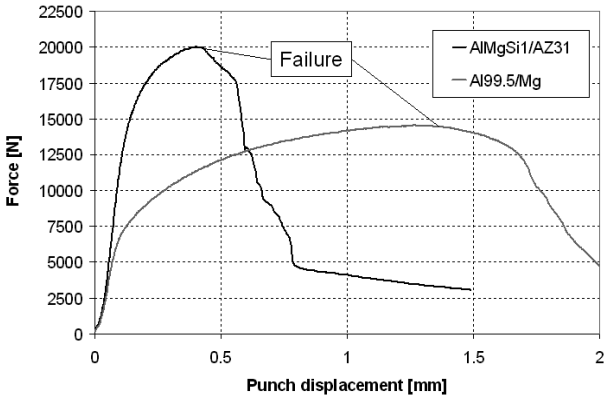

Figure 6. Punch displacement diagram, material of extrusion test 1

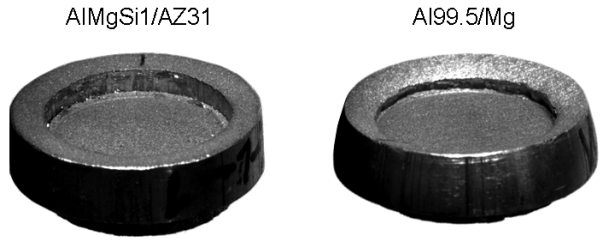

Figure 7. Specimen geometry after loading, material of extrusion test 1

Push out tests with material of extrusion experiment 2 caused relatively high failure forces. As already mentioned, the alloyed material is only partially bonded. Hence, the failure forces are lower than the force values of the unalloyed materials. In this case brittle failure occurs. The compound of the unalloyed materials shows large plastic deformation before reaching failure.

In Table 2, besides failure forces, average values of failure shear stresses are shown. These stresses are calculated by the quotient of failure force and area of shearing at the interface.

Due to variation of the compound properties in longitudinal direction of the co-extrusion rods, the forces and shear stresses apply to sections with a maximum of bonding strength. The shear stress values of the compound of the alloyed materials can not be calculated because of ramified cracks at the interface (extrusion test 1) and the partially bonding (extrusion test 2). Nevertheless a high loading capacity at the bonded parts is indicated for the alloyed materials of extrusion test 2. This will be demonstrated in section 4 of this paper.

Table 2. Failure forces and average shear stresses, determined by push out tests

Extr. test No.	Material	Failure force [kN]	Average shear stress [N/mm^2]
1	AlMgSi1/AZ31	20	–
	Al99.5/Mg	14.5	≈ 60
2	AlMgSi1/AZ31	12	–
	Al99.5/Mg	12.7	≈ 65

4. BENDING TESTS IN AN EXTENDED TEMPERATURE RANGE

4.1 Experimental setup

Besides push out tests at room temperature, which were used to investigate the behaviour of the compound under shear stress and to determine average failure shear stresses of the interface, bending tests in an extended temperature range were realized. By means of these tests, normal stress values for the interface strength are determined. Furthermore, it is possible to analyze the deformation behaviour of the interface.

The manufacturing of the small specimens was made by wire eroding with following grinding. The specimens were separated from the bonded parts of the compounds in the middle (concerning the length) of the bimetal rod. In Figure 8 the position of the bending specimen for the separating process is given. For the bending tests, material of extrusion test 2 was used.

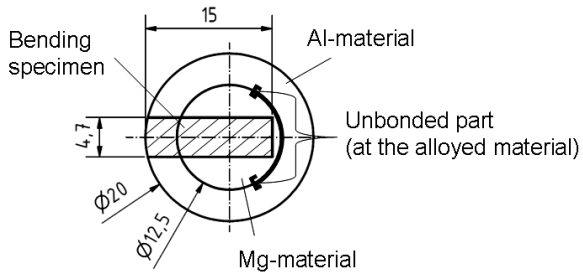

Figure 8. Position of the bending specimen in the cross-section of the co-extrusion rod

The experiments were also realized in a ZWICK testing machine. A specially developed device enables the investigations from room temperature to 400 °C, Fig. 9. This device consists of a gas heater with a temperature chamber at the front side and special components for loading. Air is used as the gas for heat transfer. A ventilator at the cold side of the device is suctioning the air. Heating of the transfer medium is realized by a resistance heating system. The hot air flows into the chamber and circulates around the loading device and the specimen. The air leaks out of the chamber through a special slot at the bottom. The force transmission is realized by ceramic punches and special components made of heat resisting steel. Ceramic is necessary for the thermal isolation. Therefore, the device can be used universally as a basis

for different tests. The special bending device is shown in Figure 10. Through a viewing glass in the front of the temperature chamber the test procedure is documented by CCD-camera images.

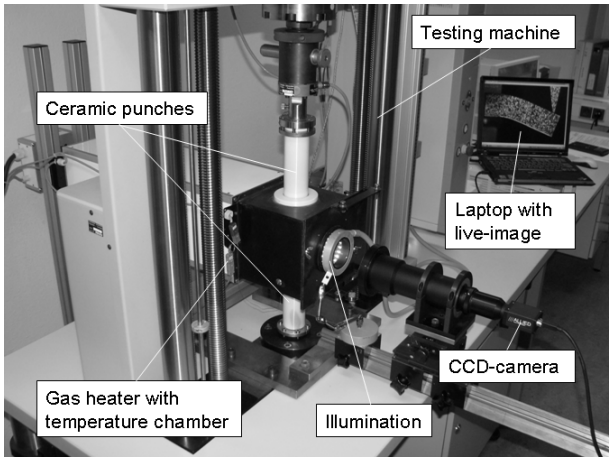

Figure 9. Experimental setup

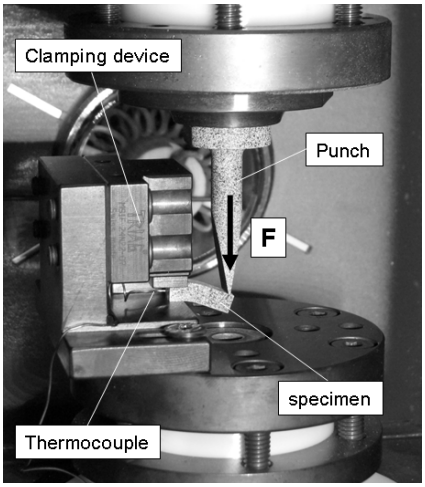

Figure 10. Bending device inside the temperature chamber

The bending load is realized by a clamp which is fixing the sleeve material (Al, Al-alloy) and a punch which is pushing the core material (Mg, Mg-alloy), Fig. 11. Because of the present load case, the shear force at the interface is unequal to zero. However, the maximum of the shear stress is located in the middle of the height of the specimen and the value is low, compared with the bending stress. Hence, failure occurs due to the maximum of the bending tensile stress at the interface $\sigma_{\text{bmax IF}}$. The theoretical linear strain distribution, which applies for the elastic range, is illustrated in Figure 11. The black and white coating on the surface of the specimen is necessary to improve the deformation analysis by Digital Image Correlation, which is described in detail in section 4.3. The bending experiments were realized at different temperatures and loading rates (punch velocity), Tab. 3. Each parameter combination was tested by 2 to 4 experiments.

Table 3. Program for the bending tests

Temperature [°C]	RT	100	200	300	400
Punch velocity [mm/min]	0.2, 20 and 200				

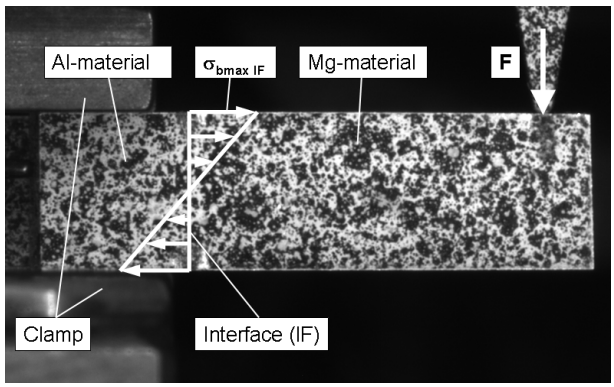

Figure 11. Bending specimen (size: $w \times h \times l = 4.7 \times 4.3 \times 15$)

4.2 Results of the interface bending strength

The failure of the bending specimens depends on the temperature, the loading rate and the co-extruded materials. One failure phenomenon is an abrupt fracture at the interface, nearly without plastic deformation before reaching failure. Another one is failure by large plastic deformation without fracture at the interface. Failure with large deformation and following fracture occurs rarely.

The calculation of maximum interface stresses at the point in time of failure was done in different ways. In case of abrupt failure (nearly without plastic deformation) the stresses are calculated by the elementary bending theory, combined with a correction factor which is determined by an elastic finite element analysis. The relation is given by (1). M_b is the bending moment, calculated by the product of the maximum force and a lever of 9.5 mm between the load application and the interface at the side surface of the specimen. The values w and h are the width and the height of the specimen.

$$\sigma_{\text{bmax IF el}} = K \cdot \frac{6 \cdot M_b}{wh^2}. \qquad (1)$$

The correction factor K equals 1.16 and is caused by the difference of the boundary conditions from an ideal fixation and the curved shape of the interface inside the specimen. The basis of the calculation of K is the hypothesis of the beginning of interface fracture in the middle of the specimen.

The finite element analysis is realized with a monolithic specimen, consisting of aluminium material. Thus an average stress is calculated without consideration of the exact, complicated stress distribution at the interface of a bimaterial specimen. The model and results of the 3-dimensional FE-analysis of the bending test are shown in Figure 12.

Because of the symmetry to the *xz*-plane a half of the specimen is modelled. The stress in Figure 12 is calculated for an example of loading with a force of 150 N. It could be proved in an experimental way that the sleeve material (Al) is slightly tilting and deforming inside the clamp. Thus, the material at the bottom is pushed on the edge of the clamp. On the upper side only the rear part is in contact with the clamping plate. Hence, the displacement boundary conditions ($u_x = u_z =$

0) at the bottom of the specimen inside the fixing section are concentrated on a narrow area. On the top, a selection of nodes (1.5 mm wide area at the rear part of the specimen) are fixed only in z direction ($u_z = 0$). This behaviour of the specimen can be interpreted as advantageous, because the interface on the tension side of the specimen is almost not influenced by the clamp. Figure 13 demonstrates that the neutral fiber is located approximately in the middle of the height of the bending beam. Therefore, it is proved that (1) can be used to determine the stresses at the interface. Although there are differences between the positive values of the normal stresses on the tension and the compression side. These differences are caused by the boundary conditions in the near of the interface on the compression side. The stresses are plotted for the already mentioned example (Force 150 N).

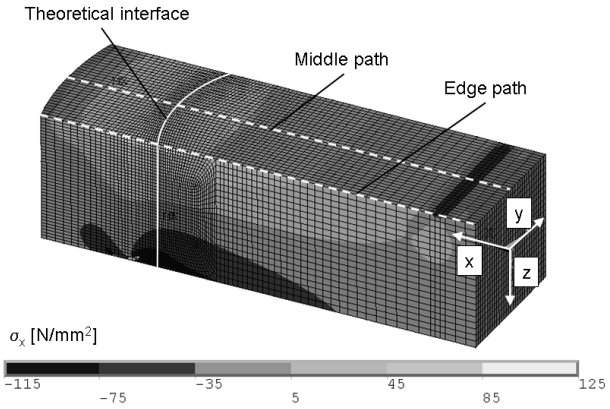

Figure 12. FE Model and strain distribution σ_x (*x*,*y*,*z*)

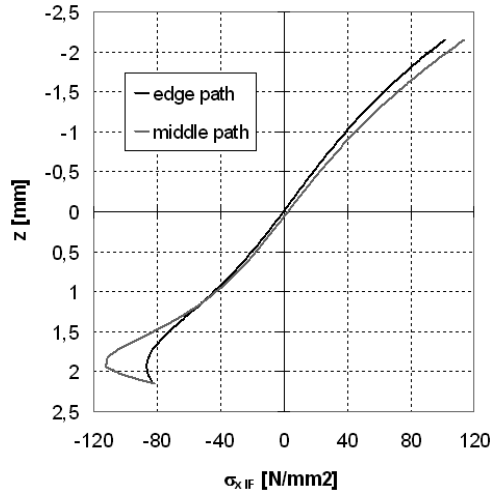

Figure 13. Strain distribution σ_x (*z*) at the interface

In Figure 14, a comparison between the normal stresses on the tension side of the solution of the FE-model (real geometry and the more exact boundary conditions) and the solution of the elementary bending theory ((1) with $K = 1$) is given. The sections of load application and fixation are not shown because of the singularities at the concerning nodes. The quotient of σ_x and $\sigma_{xn\ IF}$ is plotted versus the x coordinate. The stress $\sigma_{xn\ IF}$ presents the stress (at the edge path) at the point of the interface (IF), which is calculated by the equation of the elementary bending theory. In the section between $x = 3$ mm and $x = 8$ mm, the shape of the FE stress curves in the middle and on the edge are nearly identical to the solution of the elementary bending theory. Due to the variance of the boundary conditions from the model of an ideal fixation, the FE stresses near the interface are higher than those which are determined by the elementary bending theory. The factor $K = 1.16$ can be read off the diagram in Figure 14.

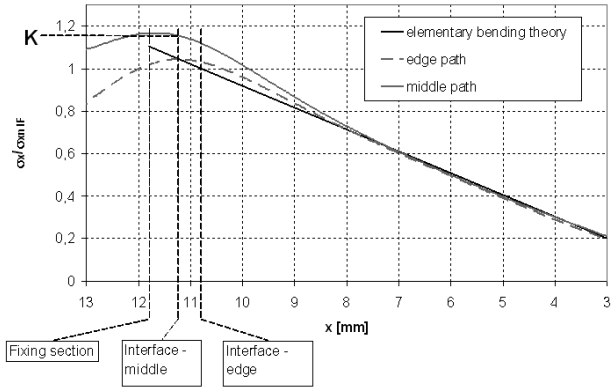

Figure 14. Strain distribution σ_x (x) on the tension side of the specimen

In the case of large plastic deformation and of failure with preceded plastic deformation, the interface bending stress is approximately determined by a calculation with fully plastic cross-section [5] and the correction factor K, (2).

$$\sigma_{\mathrm{bmax\,IF\,pl}} = K \cdot \frac{4 \cdot M_{\mathrm{b}}}{wh^2} . \qquad (2)$$

If failure with fracture at the interface occurs, the calculated stresses according to the described methods can be referred to as the interface strengths. The maxima of interface strengths of the alloyed materials reach high values from 115 to 140 N/mm, Fig. 15. The stresses are average values of 2 to 4 single tests respectively. Due to a variation of bonding properties in longitudinal direction of the co-extrusion rod, the calculated bending strengths are subject to deviation. A significant decreasing of the bending strength is proved only at temperatures of 300 °C. By Figure 15 the viscoplastic properties (especially of the AZ31 alloy) [6] are considerably demonstrated. At loading rates of 0.2 mm/min and temperatures above 300 °C, fracture does not occur. In these cases the bending strength of the interface is higher than the yield stresses of the basic materials. The differences between the determined strength values at the elevated loading rates and high temperatures are supposed to be caused by the viscoplastic properties of the basic materials. A dependency of the bending strength on the loading rate at lower temperatures (room temperature to 200 °C) can not be demonstrated.

In Figure 16 it is shown that the determined values for the interface bending strength of the Al99.5/Mg compound at temperatures until 100 °C are high (90 to 100 N/mm^2). The stresses are average values of the single tests. The yield stresses of the basic materials are lower than those of the AlMgSi1/AZ31 compound. Thus, at higher temperatures, interface fracture could not be induced. From this it follows that at elevated temperatures, the interface strength is higher than the

yield stresses respectively. The viscoplastic properties of the basic materials can be also proved.

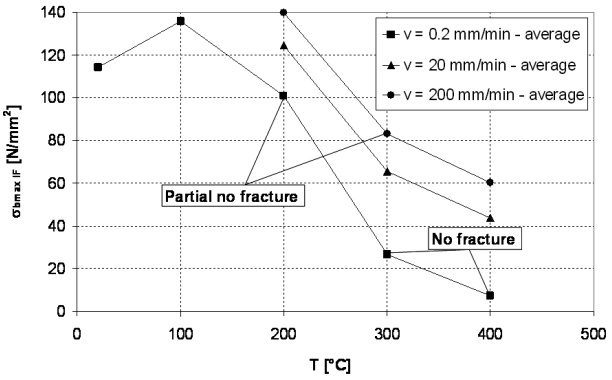

Figure 15. Maximum of interface bending stress vs. temperature, alloyed materials of extrusion test 2

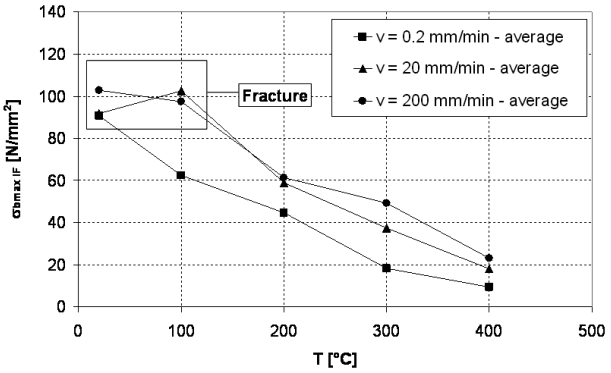

Figure 16. Maximum of interface bending stress vs. temperature, unalloyed materials of extrusion test 2

Typical results of specimen geometry after loading are given in Figures 17 and 18. Failure by brittle fracture is represented in the example of Figure 17. The specimen shows almost no plastic deformation. The surfaces of the interface show grooves in the direction of extrusion.

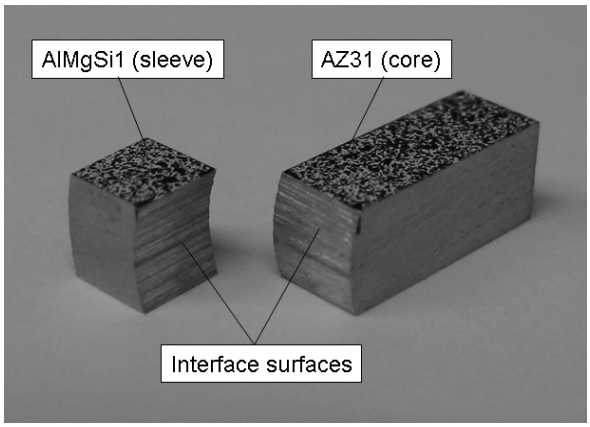

Figure 17. Bending specimen after loading at room temperature, v_{punch} = 20 mm/min, alloyed materials

In Figure 18 an example of failure by large plastic deformation is given. The interface stays undamaged (without fracture) and is deformed. On the top of the specimen contraction can be noticed and at the bottom the specimen shows extension of the width.

Besides high interface bending strength values of the compounds, good deformation behaviour at elevated temperatures can be demonstrated. Another important realisation is that in spite of a partially bonded compound, the bonded parts of the alloyed materials have advantageous interface properties.

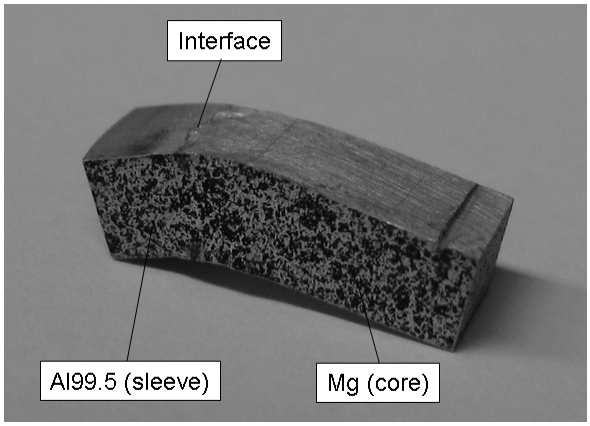

Figure 18. Bending specimen after loading at 400 °C, v_{punch} = 20 mm/min, unalloyed materials

4.3 Results of the deformation analysis by Digital Image Correlation (DIC)

The Digital Image Correlation is an optical non-contact method of digital image processing. The principle is the comparison of the grey scale values and their distribution of an image 1 (reference) and of an image 2 [7]. These two images can be assigned to different conditions, for instance unloaded and loaded. Thus the points at the surface of the specimen (represent material particles) can be recovered in the second image by a special mathematical correlation algorithm. By knowledge of the position of the material particles in condition 1 and 2, the field of the in-plane displacement can be determined. If we have the displacement fields in the form of functions, it is possible to determine the deformation field by differentiation (which will be described later). In Figure 11, section 4.1, the special coating of the specimen is shown. In the present case the subtle, chaotic distribution of black and white areas is necessary to improve the accuracy of the deformation analysis method. Heat resistant lacquer in black and white was used for the coating. The main advantage of the DIC is the applicability at high temperatures. This property is fundamental for performing the bending tests which are described in this paper. In the presented experiments, the method is used for the analysis of large deformations for which it is very well suited.

The deformation analysis was realized by using the commercial, 2-dimensional DIC system VEDDAC 4.0, which is developed and provided by the CWM GmbH, Chemnitz, Germany. For large deformations or big loading steps between the two compared conditions, a whole sequence of images should be used. This is realized in the described analysis. The so-called refresh algorithm refreshes the reference image during the displacement calculation. The interval of refreshing can be defined by the user of the software. The displacement values which are determined until reaching the actual reference image are saved and added up when reaching the next reference to get the total displacement. During the analysis a virtual, rectangular grid of dots is set on the surface of the specimen. The displacement is calculated for this defined dot matrix.

For the calculation the LAGRANGE approach is used (referring to the coordinates in the undeformed condition). Because of measuring faults, it is necessary to smooth out the measured values for the displacement fields u_x (X,Y) and u_y (X,Y). Coordinate X represents the longitudinal and Y the cross direction. For a full-field calculation this process is realized by a regression analysis, using polynomial expressions with a degree of n = 8. The number A_n of the constants a_0 … a_{An} of the polynomial expressions can be calculated by (3).

$$A_n = 1 + \sum_{m=1}^{n} (m+1) . \tag{3}$$

For n = 8, A_n equals 45. For a sufficient accurate regression analysis the number of dots has to be chosen large enough. The general equation for the polynomial expression of 8th degree is given by (4).

$$\begin{aligned} u_i(X,Y) = {} & a_0 + a_1 X + a_2 Y \\ & + a_3 X^2 + a_4 XY + a_5 Y^2 \\ & \ldots \\ & + a_{37} Y^8 + a_{38} X^7 Y + a_{39} X^6 Y^2 \\ & + a_{40} X^5 Y^3 + a_{41} X^4 Y^4 + a_{42} X^3 Y^5 \\ & + a_{43} X^2 Y^6 + a_{44} XY^7 + a_{45} Y^8 . \end{aligned} \tag{4}$$

The polynomials for u_x and u_y are used for the calculation of the deformation field. In (5) the deformation tensor of GREEN is given [8].

$$G_{jk} = \frac{1}{2}(u_{j,k} + u_{k,j} + u_{ij} u_{ik}) . \tag{5}$$

The x component G_{xx} in (6) is used to determine the aspect ratio λ_{fiber} [8] in the direction of the fiber of the specimen, (7) (fiber: line which is orientated in longitudinal direction of the specimen).

$$G_{xx} = u_{x,x} + \frac{1}{2}({u_{x,x}}^2 + {u_{y,x}}^2) , \tag{6}$$

$$\lambda_{fiber} = \sqrt{1 + 2G_{xx}} . \tag{7}$$

The logarithmic strain φ_{fiber} in the direction of the fiber can be calculated by the following equation:

$$\varphi_{fiber} = \ln \lambda_{fiber} . \tag{8}$$

The results of the deformation analysis are given by one example of a bending test. The specimen (compound of the unalloyed materials) was loaded at the temperature of 400 °C with a velocity of 20 mm/min. The calculation of the deformation is realized at a force of 29 N and a punch displacement of 1.08 mm. The measured values and the polynomial for the displacement field u_x are shown in Figure 19.

In Figure 20 the displacement field in x-direction is shown. The values of the LAGRANGE approach are plotted versus the EULER coordinates x and y (referring to the deformed condition). The black crosses represent the dots at the side surface of the specimen.

The calculated distribution of the logarithmic strain, plotted versus the EULER coordinates is presented in

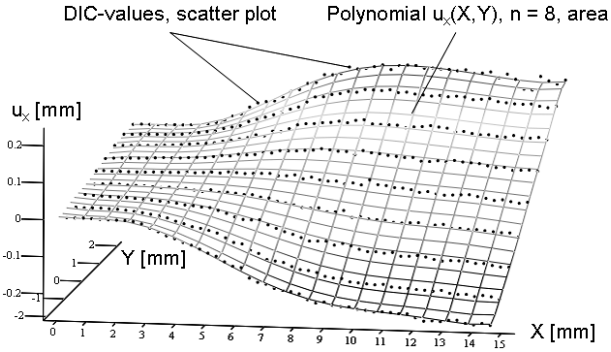

Figure 19. Measured values and smoothed polynomial function for the displacement field in *x*-direction u_x (X,Y)

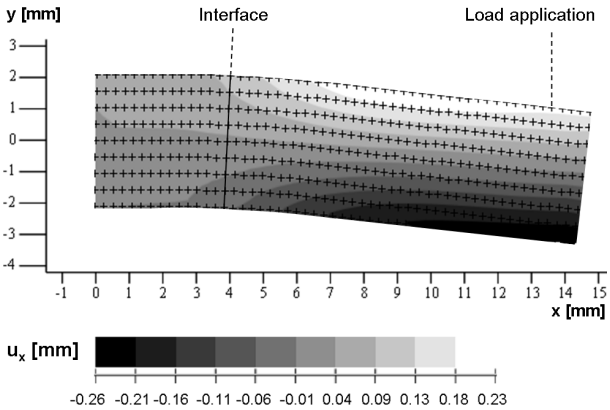

Figure 20. Polynomial function and distribution for the displacement field in *x*-direction u_x (x,y) in the *xy*-plane

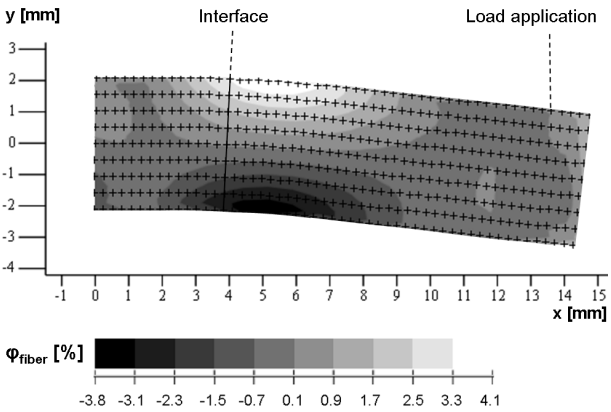

Figure 21. Strain distribution φ_{fiber} (x,y) in the *xy*-plane

Figure 21. The maximum of deformation is near the interface at the magnesium side. The strain distribution shows nearly symmetric properties. The location of the neutral fiber is approximately in the middle of the height of the specimen. Therefore, (2) can be used for the calculation of bending stresses at large deformations. The Digital Image Correlation is a very applicable method to determine the deformation behaviour of the bending specimen at high temperatures. Hence this method is applicable for verification of numeric simulations of deformation processes.

5. CONCLUSION

The investigations include experimental and numerical analyses of hydrostatic co-extruded aluminium/ magnesium compounds (co-extruded with different process parameters). By an analysis of the constitution of

the interface it has been shown that the bonding quality of the compounds is different. The compound of the alloyed materials shows a damaged interface or it is partially bonded. The unalloyed materials show a completely bonded compound. Methods like metallographic analysis, dye penetrant test and ultrasonic analysis were used to detect damaged and unbounded areas in the co-extrusion rods. In consequence of the crack detection investigations and a numerical simulation of the production process, the manufacturing of the semi-finished product was improved by reducing the temperature of the bolt and the die.

In the paper are described different experimental tests to determine mechanical properties concerning the strength of the interface between the two metals. By means of push out tests at room temperature the behaviour of the interface under shear stress is characterized. The determined average failure shear stresses of the unalloyed materials (60 to 65 N/mm^2) and failure forces of both material configurations are high. Bending tests at an extended temperature range were performed to calculate the bending strength and to characterize the deformation behaviour of the interface. An elastic finite element analysis of the bending tests was realized to determine the stress values. Thus, a correction factor for stress determination was calculated, which is used to be combined with the equation of the elementary bending theory. The results are high values of interface bending strengths at temperatures until 200 °C for the AlMgSi1/AZ31 compound (115 to 140 N/mm^2). The interface bending strength of the Al99.5/Mg compound until 100 °C can be quantified (90 to 100 N/mm^2) however at temperatures from 200 °C to 400 °C, the strength values are higher than the yield stresses of the basic materials. In spite of a partially bonded compound, the bonded parts of the AlMgSi1/AZ31 compound show high values of bending strength. Besides the strength properties, it is demonstrated that the deformation behaviour at elevated temperatures of all tested compounds is very advantageous. Furthermore, a deformation analysis by the method of Digital Image Correlation is realized. By means of an example, the displacement field and the strain distribution on the surface of the specimen is presented.

Because of the damaged sections in the compounds of the alloyed materials, the production process has to be improved further on. In addition, experiments will be realized to determine fracture mechanical properties of the aluminium/magnesium compounds.

AKNOWLEDGMENT

The authors of this paper thank the German Research Foundation for the financial support of this work within the framework of the research project SFB 692, subproject B3.

REFERENCES

[1] Riemelmoser, F., Kilian, H., Widlicki, P., Thedja, W.W., Müller, K., Garbacz, H. and Kurzydlowski., K. J.: Co-extrusion of aluminium magnesium compounds, in: Gers, H. (Ed.): *Strangpressen*, Wiley-VCH, Weinheim, pp. 248-257, 2007, (in German).

[2] Möhler, M. and Menzel, H.-U.: Co-extruding of material compounds, in: *Conference Proceedings of Technology of Producing Material Compounds by Forming – MEFORM 2004*, 08-09.03.2004, Freiberg, Germany, pp. 53-63, (in German).

[3] Lehmann, T., Naumann, J. and Stockmann, M.: Experimental analysis of aluminium-magnesium compounds, in: *Proceedings of the 25th Danubia-Adria Symposium on Experimental Methods in Solid Mechanics*, 24.-27.09.2008, České Budějovice, Czech Republic, pp. 153-154.

[4] Awiszus, B., Naumann, J., Stockmann, M., Kittner K. and Lehmann, T.: Experimental and numerical investigations of the interface of Al/Mg compounds, in: *Proceedings of the SFB 692 Kolloquium*, 26.09.2007, pp. 55-64, (in German).

[5] Kreißig, R.: *Plastic Theory*, Specialist Book Publisher, Leipzig, 1992, (in German).

[6] Yin, D.L., Zhang, K.F., Wang, G.F. and Han, W.B.: Superplasticity and cavitation in AZ31 Mg alloy at elevated temperatures, Materials Letters, Vol. 59, No. 14-15, pp. 1714-1718, 2005.

[7] Tarigopula, V., Hopperstad, O.S., Langseth, M., Clausen, A.H., Hild, F., Lademo, O.-G. and Eriksson, M.: A study of large plastic deformations in dual phase steel using Digital Image Correlation and FE analysis, Experimental Mechanics, Vol. 48 No. 2, pp. 181-196, 2008.

[8] Prager, W.: *Introduction to Continuum Mechanics*, Birkhäuser, Basel, 1961, (in German).

ЕКСПЕРИМЕНТАЛНА И НУМЕРИЧКА ИСПИТИВАЊА ОПТЕРЕЋЕЊА НА ПОВЕЋАНОМ ТЕМПЕРАТУРСКОМ ОПСЕГУ КОД УЗОРАКА ЈЕДИЊЕЊА АЛУМИНИЈУМА И МАГНЕЗИЈУМА

Томас Лехман, Мартин Штокман, Јохен Науман

Рад представља део пројекта који има за циљ испитивање чврстоће и механичких карактеристика лома хидростатичких коекструдираних једињења алуминијума и магнезијума. Приказани су основни резултати испитивања квалитета једињења и пробе оптерећења на температурама до 400 °C. Легирани материјали се само делимично везују или оштећују, док код једињења нелегираних материјала гранична површина је спојена у потпуности. Чврстоћа граничне површине се израчунава помоћу вредности за силу прелома код проба савијањем и *FE* симулацијом у условима напона на месту граничне површине. Деформационо понашање се одређује корелацијом дигиталне слике (Digital Image Correlation). Како легирани, тако и нелегирани материјали показују високе вредности чврстоће на спојеним деловима материјала. Даље, испитивањима на високим температурама може се доказати веома добро деформационо понашање без пукотина на граничној површини.